Long-term coherence of the cyclotron mode in a trapped ion cloud

A. J. Peurrung and R. T. Kouzes
Pacific Northwest Laboratory, Richland, Washington 99352
(Received 29 November 1993)

An entire family of mass spectrometers relies on the excitation and subsequent detection of the cyclotron mode in a trapped ion cloud. The observed long-term coherence of this mode is critical to the success of these instruments. This paper analyzes the dynamics of the charge cloud after excitation and finds that they are mathematically equivalent to the dynamics of the cloud before excitation. A vortex-like rotation of the cloud prevents expansion under many conditions depending on the trap geometry and the properties of the cloud. The stability of an excited ion cloud with velocity dispersion and applied shear is analyzed and numerical predictions of relevance for ion cyclotron mass spectroscopy are made.

PACS number(s): 52.25.Wz, 35.10.Bg, 82.80.Ms, 07.75.+h

I. INTRODUCTION

Ion cyclotron resonance (ICR) mass spectrometers have become the preferred instrument for a wide variety of mass measurement applications [1]. These instruments routinely achieve a precision of one part in 10^7 and can simultaneously weigh a large number of different species [2–4]. At the heart of these instruments is a Penning trap which utilizes an electric potential well and an axial magnetic field to confine ions. Precise measurements rely on excitation of the cyclotron mode in an ion cloud, and subsequent detection of that mode in such a way that the cloud remains intact for as long as possible. The excitation process has been extensively studied [5–8], and advanced techniques have been developed which permit the excitation of the cloud to a large cyclotron radius with minimal disruption. Once excited, this mode may require more than 10^6 periods to decay. This exceptionally long coherence time implies that some physical process operates to prevent the more rapid loss of the cloud's structure. This paper analyzes the excited cloud's dynamics, and proposes that it rotates in a way which provides stabilization and therefore directly results in long-term coherence.

The extraordinary stability of charge clouds in a symmetric trap has traditionally been explained as a consequence of angular momentum conservation [9]. When the trap is asymmetric or the cloud is off-center, however, an energy-based argument is required to explain the cloud's long-lived stability [10,11]. Assuming that a cloud contains a sufficient number of ions that collective effects are important, its kinetic energy prior to excitation is small compared to its self-electrostatic potential energy

$$\sum_i \tfrac{1}{2} m_i v_i^2 \ll \sum_i \tfrac{1}{2} q_i \phi(\mathbf{r}_i) \ , \tag{1}$$

where r_i, v_i, m_i, and q_i are the radius, velocity, mass, and charge of the ith ion, and $\phi(\mathbf{r}_i)$ is the potential at $\mathbf{r}_i$. It can be shown that the cloud's self-electrostatic potential energy is maximal with respect to changes in the cloud's size or shape [10]. Since the cloud's dynamics must conserve electrostatic energy, it is energetically impossible for the cloud to expand or distort [10]. It is not initially clear what becomes of this stability principle for an excited cloud. The kinetic energy from the excited ion cloud's coherent motion is generally much larger than the cloud's self-electrostatic potential energy. It is therefore possible for the cloud to expand or distort as coherent kinetic energy and electrostatic energy are exchanged. As a result, there appears to be no stability constraint on the cloud dynamics.

How does the excited charge cloud manage to retain a compact shape for detection times greater than 10^6 cyclotron periods? There are certainly effects which act to tear the cloud apart on more rapid time scales. Some ions within the cloud may follow trajectories which are distinct from the trajectories of other ions in the cloud [12]. For example, ions with different axial energies may experience different average radial electric fields. If the motion of any particle is sufficiently different, it should rapidly separate and contribute to the cloud's loss of coherence. In addition, the effective gyration frequency is usually a slight function of the radial distance to the trap center. This dependence is equivalent to a shear which may distort or even completely destroy the cloud's structure.

An excited charge cloud acquires resistance to these destructive effects as a result of a rotational motion. In the frame of reference which moves with the cloud's cyclotron motion, the cloud undergoes an additional rotation about its own center. The motion is due to the cloud's own electric field, and is therefore distinct from the cyclotron and magnetron motions. We discuss this motion below, and show how it leads to improved mode coherence in the presence of destructive effects of limited strength. This rotation is most important for high density and high mass charge clouds. This helps explain why cloud compression is critical for successful mass measurement [13], and why very long-lasting, coherent cyclotron modes are observed for high mass ions [14,15].

II. DYNAMICS OF AN ION CLOUD IN THE CYCLOTRON MODE

A review of the dynamics of an unexcited charge cloud confined within a Penning trap is needed [16]. Figure 1 shows a side view of a typical trap geometry. A uniform, axial magnetic field B and bias voltages applied to the ends of the trap combine to provide effective confinement of an ion cloud. An ion's axial, oscillatory motion due to the trap potential well does not affect its motion in the plane perpendicular to the magnetic field to lowest order. The two dominant forces which govern the perpendicular motion of an ion are the electric force from the cloud's own space charge and a magnetic force from the externally imposed magnetic field. As a result of these two forces, ions undergo $\mathbf{E}\times\mathbf{B}$ drift in the azimuthal direction around the cloud. Many physically interesting ion clouds have a shape that is approximately spheroidal, where both of the semiaxes in the plane perpendicular to the trap axis have lengths ρ_c. The cloud may have an arbitrary axial aspect ratio $\alpha=z_c/\rho_c$, where $2z_c$ is the extent of the cloud in the axial direction. The space charge from a cloud with this shape produces an electric field with the particularly simple form [17]

$$E_\rho=\frac{m\omega_i^2}{3q}a(\alpha)\rho\ , \tag{2}$$

where ρ is the radial coordinate measuring distance from the cloud center, $\omega_i^2=(nq^2/\epsilon_0 m)$ is the plasma frequency squared, and $a(\alpha)$ is a coefficient which accounts for the cloud's elongation. Since the electric field is proportional to ρ, $\mathbf{E}\times\mathbf{B}$ drift causes the cloud to rotate as a rigid rotor with a frequency

$$\omega_\rho=\frac{a(\alpha)}{3}\frac{\omega_i^2}{\Omega}\ , \tag{3}$$

where $\Omega=qB/m$ is the cyclotron frequency. The coefficient $a(\alpha)$ is obtained from

$$a(\alpha)=\frac{3}{2}\left[1-\frac{1}{\alpha^2-1}Q_1^0\left[\frac{\alpha}{\sqrt{\alpha^2-1}}\right]\right]\ , \tag{4}$$

where Q_1^0 is the associated Legendre function of the second kind. Note that Eq. (4) has two different forms valid when α is greater and less than one [17,18]. Although Eqs. (2)–(4) cannot be applied to an ion cloud with a cross section that is far from circular, they provide a useful approximate description of the motion of clouds with shapes that are close to the assumed form.

A second basic motion in an ion cloud is bulk, coherent cyclotron motion of the entire cloud about some point other than the cloud center. The exact frequency at which this cyclotron gyration occurs is $\omega_+=\Omega-\omega_D$, where ω_D is the drift frequency that results from the trap and image electric fields [19,20]. This drift frequency is known alternately as the magnetron or diocotron frequency depending on whether the trap or image fields are of dominant importance [14,15,21,22]. If the rotational center of the cyclotron motion is any point other than the trap center, this point will also drift around the center with a frequency ω_D. For the purposes of this paper, it is acceptable to ignore all forms of this magnetron motion so that the effective cyclotron frequency ω_+ is approximated as Ω. The relaxation of this assumption might alter the details of the system's dynamics, but will not invalidate the basic physical effects described below (provided $|\omega_D|\ll|\Omega|$).

Cyclotron motion can be driven to any amplitude depending on the strength and duration of the external electric fields used for excitation. Although this mode has been observed in electron clouds [19,20], it is much more commonly used with ion clouds for mass spectrometry. It does not matter that the cloud undergoes a slow $\mathbf{E}\times\mathbf{B}$ rotation about its own center; the linearity of the Lorentz force equation implies that the two motions must coexist in a single cloud. Further insight can be gained by viewing the dynamics from a frame of reference which gyrates with the cloud about the trap center but does not rotate. In this frame, the magnetic and inertial forces involved in the cyclotron gyration are absent. The remaining electric and magnetic forces cause the cloud to rotate in a manner identical to that of the unexcited cloud.

Figure 2 illustrates the cloud's motion before and after

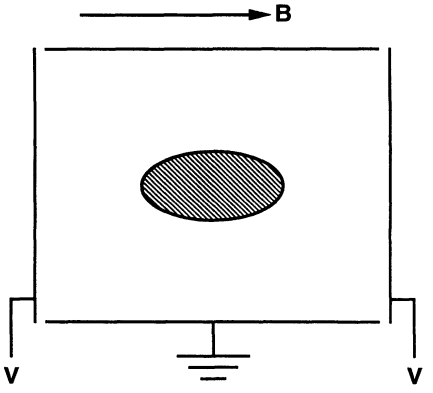

FIG. 1. Side view of a typical trap geometry.

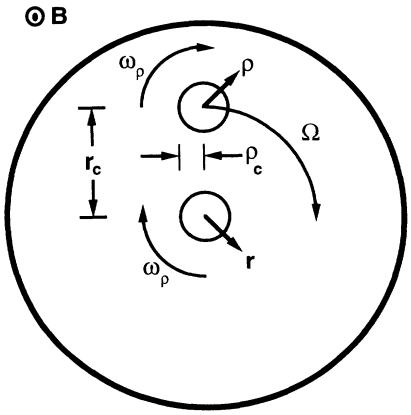

FIG. 2. Axial view of cloud motion geometry. The unexcited cloud is shown at the trap center and rotates at a frequency of ω_ρ. The excited cloud rotates about its own center at the same frequency while simultaneously undergoing cyclotron motion about the trap center.

the excitation of a large-amplitude cyclotron mode. For a magnetic field as shown, an unexcited cloud of positively charged ions will rotate at ω_ρ. The excited cloud has two collective motions: (1) a coherent gyration about the trap axis at Ω, and (2) a rotation at ω_ρ about its own central axis. Although the rotation may be much slower than the cyclotron gyration, it ensures that the cloud does not always keep the same orientation within the trap. The ratio of the excited cloud's rotation and gyration frequencies is

$$\frac{\omega_\rho}{\Omega}=\frac{a(\alpha)}{3}\frac{\omega_i^2}{\Omega^2}\ . \tag{5}$$

Disregarding factors of order 1, this ratio is equal to the factor by which the charge cloud is below its Brillouin confinement limit, $\omega_i^2/2\Omega^2=1$ [23].

The above analysis predicts more than the rotational motion of the cloud. Any and all dynamics of the excited cloud in the frame of reference that gyrates with the cyclotron motion are *identical* to the dynamics of an unexcited cloud. Any analytical tools used to understand the motion of unexcited ion clouds are also applicable to excited clouds. For example, if the cloud has a constant density within an elliptical region, there is an analogy which relates its behavior to the behavior of a vortex in a two-dimensional, inviscid fluid [24–26]. This analogy uses the fact that if the charge density and electrical potential of the cloud are identified with the vorticity and stream function of the fluid, the equations governing their dynamics are identical. This powerful analogy may help in the solution of more complex problems such as the interaction of multiple-ion clouds of different mass particles. Section III analyzes the effect of an externally imposed shear on the long-term coherence of an excited charge cloud with the help of the fluid analogy.

III. CLOUD STABILIZATION

The cloud's rotation is an important physical process which may prevent the rapid expansion and consequent loss of ICR signal. Unlike an unexcited charge cloud, the excited cloud may expand or dramatically distort while conserving total energy. Within certain limits, which we set forth below, the rotational motion stabilizes the cloud.

There are two categories of effects which can lead to cloud expansion. The first category of effects causes different particles within the cloud to have different effective gyration frequencies. One such effect would be the presence of particles of two or more different masses. The second category of effects exerts a shear on the charge cloud. These effects usually arise from imperfections in the trap design which cause the cloud's gyration frequency to depend slightly on position.

A. Individual particle velocities

In general, anything which differentiates the ions within an excited charge cloud may give each of them an individual velocity relative to the cloud as a whole. For example, the ions may have a variety of masses, charge states, or axial energies. For this analysis, the effective gyration frequency of one ion in the cloud is assumed to differ by $\delta\Omega$ from all of the other ions in the cloud. If $\delta\Omega$ is 0, this ion executes a circular orbit around the center of the cloud as a result of the cloud's rotation. Clearly, if $\delta\Omega$ is sufficiently large, then the ion escapes from the cloud's influence and is effectively lost. If a number of ions are lost in this manner, the cloud quickly expands and mode coherence lasts only for a short time.

An estimate for the individual velocity needed to escape from the cloud is obtained by equating the cloud rotation time to the time an ion requires to traverse the diameter of the cloud at its individual velocity

$$\frac{2\pi}{\omega_\rho}=\frac{2\rho_c}{r_c\delta\Omega}\ , \tag{6}$$

where ρ_c is the cloud's radius and r_c is its gyration radius. This relation can be expressed as $v_i=v_e/\pi$, where v_i is the individual velocity of an ion in the cloud, and v_e is the velocity of an ion at the edge of the cloud due to the cloud's rotation.

An improved, secondary estimate for the ion velocities that lead to rapid cloud expansion and loss of coherence is obtained by direct computation of ion trajectories. Figure 3 shows the geometry for this calculation in the frame of reference that moves with the cloud's gyration. In this frame of reference, the ion cloud's center is stationary. The x and y coordinates measure distance in the plane perpendicular to the trap axis, and $\hat{\mathbf{x}}$ is the direction of the ion's individual motion. The cloud as a whole rotates at a frequency ω_ρ, and an ion at position A is assumed to have an independent velocity $v_i=r_c\delta\Omega$. Position A is the location at which a particle is most likely to escape since it begins at the edge of the cloud, and its individual velocity (assumed to be toward the right) moves it radially outward for a maximum amount of time. The cloud is assumed to be initially circular and to have a constant density within its spheroidal volume. The motion of ions is studied only in two dimensions, and the

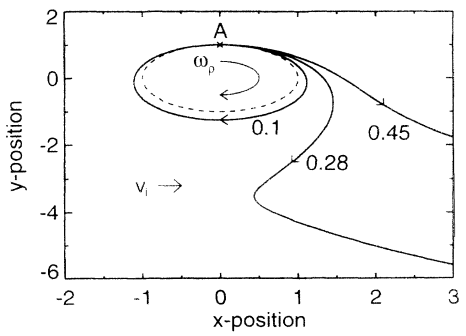

FIG. 3. Trajectories of individual ions in the frame rotating with the cloud at Ω for $v_i/v_e=0.10$, 0.28, and 0.45. The outer edge of the circular ion cloud is represented by the elliptical dotted line in these coordinates. The vortex rotates clockwise at a frequency of ω_ρ in this frame of reference. All positional coordinates are normalized to the cloud's radius. Each trajectory starts at position A.

cloud's radial electric field is assumed to fall off as $E_\rho(\rho) \propto \rho_c/\rho$ for positions outside the cloud's radius, ρ_c. These approximations should be reasonable for the region near the charge cloud. Particles without escape velocity are unlikely to leave this region.

Figure 3 shows the trajectories of an ion initially at position A for several different ratios of its individual velocity to its rotational velocity. A particle executes a closed orbit when

$$v_i < 0.28 v_e \ , \tag{7}$$

where $v_e = \omega_\rho \rho_c$ is the rotational flow velocity at the cloud's radial edge. For larger values of this ratio, however, the particle escapes from the cloud. For ions at other initial positions, the coefficient in Eq. (7) is larger, reaching a maximum of 0.6 for an ion that begins at the cloud center. Cloud coherence, however, is determined by Eq. (7) because whenever ions at the edge of the cloud are lost, it becomes easier for the interior ions to escape. Whenever substantial numbers of ions fail to satisfy Eqs. (7), the cloud "evaporates" in a time which is of the same order as the rotation time. If, however, the vast majority of cloud ions satisfy Eq. (7), then we conclude that the cloud is stable and coherence is long-lived. If a large number of ions barely satisfy the stability condition, they undergo highly elliptical orbits, and the ultimate fate of the cloud is unclear.

B. Imposed shear

Possible sources of shear for an ion cloud that undergoes cyclotron motion include anything which results in a dependence of the exact gyration frequency on the position within the trap. If the cloud is not too close to the trap center, an imposed shear flow with vorticity s can be written approximately as

$$v_x = -sy \ , \tag{8}$$

$$v_y = 0 \ , \tag{9}$$

where the frame of reference is chosen so that v_x and v_y are ion velocities along and perpendicular to the shear direction, respectively. Possible sources of shear are magnetic-field inhomogeneities [27], image charge effects [18,22,28], passive space charge at the trap center, and nonharmonic or asymmetric components of the trap's electrical potential well [29,30]. Inhomogeneities in the rf electric field may also exert a shear on the ion cloud during excitation. Two points at opposite ends of a cloud diameter along the y axis have a relative velocity of $2s\rho_c$. Equating this relative velocity with the rotational velocity of the cloud's edge allows us to derive a crude estimate of the shear required to rapidly destroy cloud coherence

$$\frac{|s|}{2\omega_\rho} = \frac{1}{4} \ , \tag{10}$$

where $2\omega_\rho$ is the vorticity of the cloud's rotational flow.

We utilize the fluid analogy for an improved analysis of the effect of shear on the ion cloud. This analysis is intended only to reveal the general properties of an ion cloud undergoing shear and rotation, and not to provide a highly accurate stability limit. According to the fluid analogy, the uniform density charge cloud can be viewed as a rigidly rotating vortex in a two-dimensional, inviscid fluid. Kida [31] studied the time-dependent behavior of a uniform vortex with an elliptical shape and found the magnitude of shear beyond which the vortex is no longer stable. If the shear is too strong, then the vortex is quickly stretched into a thin line and effectively destroyed. If, however, the shear is not too strong, the cloud is stable and cannot be torn apart even after a very long time. Although the fluid analogy for a three-dimensional cloud is exact only when the cloud has a circular cross section in two dimensions, stable clouds tend to remain roughly circular, and therefore the fluid analogy is approximately valid.

The necessary condition for long-term stability found by Kida is

$$\frac{s}{2\omega_\rho} > 2\sqrt{2} - 3 \approx -0.17 \ . \tag{11}$$

Although a vortex may be stable, its two-dimensional aspect ratio λ oscillates on a time scale which normally is comparable to the vortex rotation frequency. We studied these oscillations for an initially circular ($\lambda = 1$) vortex by numerical integration of Kida's equations for the evolution. Figure 4 shows the minimum aspect ratio reached during the course of the oscillations as a function of shear strength. The numerically observed limit of long-term stability is approximately $s/2\omega_\rho > -0.148$, which is close to the absolute limit in Eq. (11). For $s/2\omega_\rho > 1.0$, however, the vortex reaches a sufficiently elongated state that the fluid analogy probably ceases to be valid, and the ion cloud is at risk of destruction. Certainly for $s/2\omega_\rho > 2.0$, the cloud becomes so elongated that Eqs. (2)–(4) cease to apply, and the cloud's rotational motion is greatly slowed. The cloud in this case is stretched without limit and destroyed. Notice that an ion cloud is more easily destabilized by a shear with adverse vorticity ($s < 0$). There is a range of shear strengths for which destabilization occurs only if the shear is opposed to the vortex rotation.

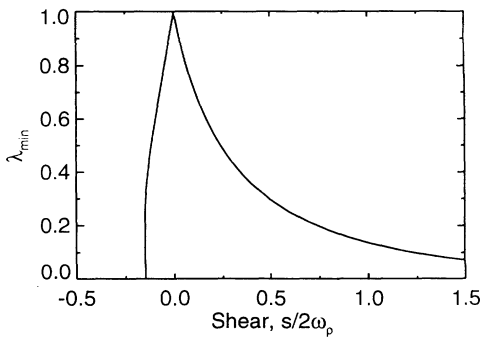

FIG. 4. Minimum aspect ratio λ vs shear strength for a two-dimensional charge cloud. The shear is quantified by the ratio of the vorticity of the shear flow to the vorticity of the cloud's rotational flow. The cloud's shape is circular for $\lambda = 1$, and becomes increasingly elliptical as λ goes toward zero.

IV. IMPLICATIONS FOR MASS SPECTROSCOPY

Equations (3), (7), and (11) determine the stability of any given excited charge cloud once the trap geometry and its imperfections are completely known. The primary result is that an ion cloud is more stable if its rotation rate increases or the magnitude of shear and individual particle velocities decrease. Because the magnitudes of the destructive effects are often proportional to the cyclotron frequency, the two stability conditions, Eqs. (7) and (11), can be expressed as $\omega_\rho/\Omega > \epsilon$, where $\epsilon \ll 1$ represents the strength of destructive effects and ω_ρ/Ω is given by Eq. (5). This analysis predicts that cloud stability is reduced as the magnetic-field strength is increased. Experimentally, clouds may actually be more stable at higher magnetic fields if they can be formed more compactly.

An interesting conclusion that can be drawn from our stability analysis involves mass and charge dependence. The cloud's slow $\mathbf{E}\times\mathbf{B}$ rotation frequency ω_ρ depends linearly on charge but is nearly independent of mass. The cyclotron frequency, of course, depends on the ion's charge-to-mass ratio. Equation (4) therefore predicts that cloud stability increases with mass. Experimental observations have shown that the cyclotron mode in a high mass ion cloud can persist for a long time [14,15]. Figure 5 shows the stability ratio ω_ρ/Ω for a typical ion cloud as a function of the ion's mass. For numerical examples from here on, we assume that a typical ion cloud with 10^4 ions is spherical and has a radius ρ_c of 1 mm, and is located at $r_c = 1.0$ cm inside a trap with a magnetic field of 7 T.

Since the rotation frequency depends linearly on the density of ions within the cloud, high-density clouds should be inherently more stable. Experimental results have indicated that longer transients and improved mass measurements are obtained when the cloud is as compact as possible [5,13]. If compaction occurs in such a way that shape and total charge are preserved, then the cloud's stability improves as the inverse cube of its size. Axial compaction can also improve stability. Figure 6 shows the rotation frequency as a function of the axial elongation α of a cloud of constant charge. Note that as the cloud becomes infinitely oblate ($\alpha = 0$), the rotation frequency reaches a limiting value of $3\pi/4$ times the rotation frequency of a spherical cloud ($\alpha = 1$). Concentration of the cloud's space charge has other beneficial effects for mass spectrometry. For example, a reduction of the cloud's physical size generally reduces the cloud's initial velocity dispersion and reduces the dispersion caused by inhomogeneous electric fields during excitation.

A cloud is most vulnerable to shear along a direction perpendicular to the trap axis, which we designate as the x axis. Although there may be radial shear within the trap, the cloud rotates at $\omega_\rho \approx \Omega$ in the frame which gyrates about the trap center with the cyclotron motion. This rapid rotation provides stability against radial shear. The shear strength can be written $s = r_c \delta\Omega/\rho_c$, where $\delta\Omega$ is the variation of the effective gyration frequency across the radius of the charge cloud. Using Eq. (11), the cloud's stability condition is then written approximately as

$$\frac{\omega_\rho}{\Omega} > 3\left[\frac{r_c}{\rho_c}\right]\left[\frac{\delta\Omega}{\Omega}\right]. \tag{12}$$

Assuming that $m = 1000$ u and $q = 5e$, where e is the charge on the electron, Eq. (5) yields the value $\omega_\rho/\Omega = 0.015$. The maximum tolerable variation in the cyclotron frequency across the cloud's radius is therefore $\delta\Omega = 5.1\times10^{-4}\ \Omega$. The magnetic-field inhomogeneity over the entire volume of a typical ICR cell corresponds to roughly $\delta\Omega = 10^{-5}\ \Omega$ [27]. Most sources of extraneous electric fields in the cell, such as space charge, image charge, and nonharmonic components of the trapping field, also do not produce a shear of this magnitude. Shear is thus quite unable to affect the coherence of the cyclotron mode in this particular ion cloud.

The stability limit arising from the individual motion is given by Eq. (7). If a cloud consists of two species with

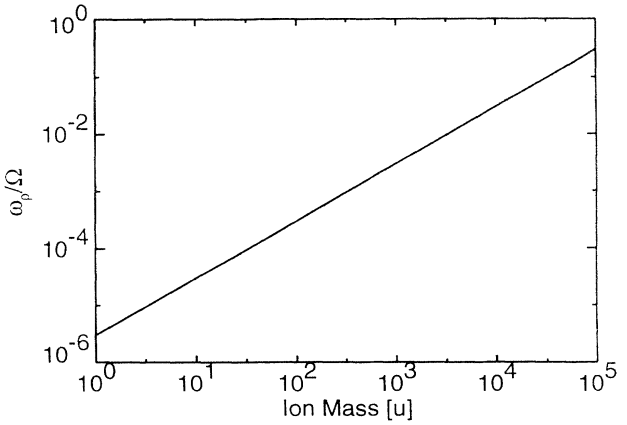

FIG. 5. Ratio of the cloud rotation frequency ω_ρ to the cyclotron frequency Ω vs ion mass for a typical ion cloud. High mass ion clouds are substantially more stable. A cloud with the assumed parameters is below the Brillouin limit when $m < 2\times10^5$ u. Clouds consisting of high-mass ions can only be formed at lower ion density.

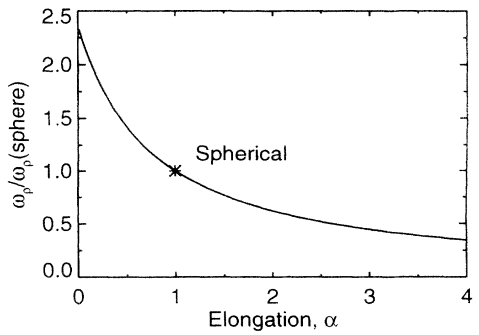

FIG. 6. Rotation frequency of the ion cloud vs axial cloud elongation. The total charge in the cloud is assumed to be constant. The angular rotation frequency is normalized to the frequency of a spherical cloud. The cloud is a sphere for $\alpha = 1$, an axially flattened disk for $\alpha = 0$, and a cylinder for $\alpha = \infty$.

masses that differ by the small quantity δm, then the individual velocity of the ions is $v_i = \Omega r_c \delta m / m$. The coherent flow velocity at the edge of the vortex is $v_e = \omega_\rho \rho_c$. The stability limit in Eq. (7) therefore becomes

$$\frac{\omega_\rho}{\Omega} > 3.6 \left[\frac{\delta m}{m} \right] \left[\frac{r_c}{\rho_c} \right] . \tag{13}$$

For the typical ion cloud described above, the cloud stability is lost when the mass difference exceeds $\delta m / m = 4.3 \times 10^{-4}$. Since this condition is nearly always satisfied, an ion cloud composed of multiple species should immediately break up into separate clouds each consisting of a single species. If this cloud is to remain stable, there must also be a limit on the possible variation of the axial "bounce" frequencies ω_z of the ions. An ion with an axial frequency that differs by $\delta\omega_z$ from the remainder of the cloud will have a cyclotron frequency which differs by

$$\delta\Omega = \frac{\omega_z \delta\omega_z}{\Omega} . \tag{14}$$

Equation (14) is derived using the relation $\Omega^2 = \omega_z^2 + \omega_+^2$ [18], where ω_+ is the effective gyration frequency of the cloud inside the trap, and ω_+ is replaced with Ω to lowest order. The stability limit for this case can therefore be expressed as

$$\frac{\omega_\rho}{\Omega} > 3.6 \left[\frac{r_c}{\rho_c} \right] \left[\frac{\omega_z \delta\omega_z}{\Omega^2} \right] , \tag{15}$$

or equivalently as

$$\frac{\delta\omega_z}{\omega_z} < 0.28 \left[\frac{\rho_c}{r_c} \right] \left[\frac{\omega_\rho \Omega}{\omega_z^2} \right] . \tag{16}$$

With the typical cloud parameters assumed above, and a trap with a primarily harmonic potential well that is 5 cm long and 1 V deep, the angular axial oscillation frequency is approximately 1.75×10^4 s^{-1}. The stability limit in this case is $\delta\omega_z / \omega_z < 0.63$. This typical cloud is therefore stable in any trap potential well that is sufficiently harmonic that $\delta\omega_z \ll \omega_z$.

The particular ion cloud used above for a numerical example is completely stable. The cyclotron mode in such a cloud would remain coherent until effects not considered in this paper cause a gradual loss of coherence. Examples of such effects are transport arising from collisions with neutral molecules or the loss of ions out of the axial ends of the trap. Additionally, the interaction between different clouds within the same trap may cause expansion and loss of coherence.

V. THE FAST ROTATIONAL MODE

As a final topic we discuss the stability of an ion cloud that undergoes fast rotational motion about its own center. In addition to the slow, $\mathbf{E} \times \mathbf{B}$ rotational mode described by Eq. (3), there is a fast mode in which every ion undergoes cyclotronlike motion about the cloud center at an angular frequency of $\Omega - \omega_\rho$ [23]. The downshifting of the cyclotron frequency is understood by considering the frame of reference which rotates about the cloud center at the cyclotron frequency. In this frame, the cyclotron motion vanishes, and the cloud has the same electric and magnetic forces which cause $\mathbf{E} \times \mathbf{B}$ rotation in the slow mode. However, this frame's rotation causes a new Coriolis force which is twice as strong as the magnetic force but opposite in direction. As a result, the ions rotate about the cloud center under the combined influence of the Coriolis and magnetic forces at the frequency ω_ρ, but in the opposite direction from the slow mode rotation. Which rotational mode a given ion cloud is in depends on its experimental history [32]. Experimental studies have confirmed the expected downshifting of the fast rotation frequency using an electron beam which enters the fast mode when it passes through a magnetic cusp (a point where the field direction reverses) [33]. Generally, any process which adds sufficient angular momentum to the ion cloud leaves it in the fast mode. Like the slow rotational mode, the fast rotational mode can be combined with bulk cyclotron gyration of the cloud about the trap center. The frame of reference that is most useful for analyzing these combined motions is the frame which rotates about the trap center at the cyclotron gyration frequency Ω. Note that in this case the frame rotates as it gyrates. This frame follows the cloud's gyration and most of its self-rotation. The cloud is stationary in this frame except for a slow counter-rotation at ω_ρ which results from the downshifting of the fast rotational frequency.

The destabilizing effect of individual ion motions on this cloud is the same as described above because nothing is different except the direction of the cloud's rotation. The type of shear which most affects this cloud's stability, however, is radial shear. Image charge, passive space charge at the trap center, and trap field errors all contribute directly to radial shear. It is likely, therefore, that the coherence of the cyclotron mode would be substantially less long lived for a cloud in the fast rotational mode.

VI. CONCLUSION

The dynamics of an excited charge cloud are formally identical to the dynamics of an unexcited charge cloud. A powerful analogy therefore relates the excited cloud's behavior to that of a two-dimensional vortex in an inviscid fluid. An important feature of this dynamics is the rotation of the charge cloud in the frame of reference that moves with the cyclotron motion. This rotation may be responsible for the experimentally observed long-term coherence of the cyclotron mode. Both individual particle effects and externally imposed shear destabilize the cloud only when strong enough to overcome the effect of the cloud's rotation.

Although the numerical limits derived in this paper are

intended to be only approximate, this treatment should serve as a guide for understanding long-term coherence. It is now possible to analyze the relative stability of different types of charge clouds in various trap geometries. Stability is optimized for cool, compact, high-density clouds and ions with a high mass. An ion cloud is stable only when the masses of the cloud's ions are sufficiently close in value. Future experiments may exploit this understanding of the cyclotron mode to deliberately enhance coherence and thereby improve the accuracy and resolution of mass measurements.

ACKNOWLEDGMENTS

We thank Steve Barlow and Fadel Erian for stimulating discussions on the subject of this paper. This research was supported by the Northwest College and University Association for Science (Washington State University) under Grant No. DE-FG06-89ER-75522 with the U.S. Department of Energy. Pacific Northwest Laboratory is operated by Battelle Memorial Institute for the Department of Energy under Contract No. DE-AC06-76RL0 1830.

[1] *Analytical Applications of Fourier Transform Ion Cyclotron Resonance Mass Spectrometry,* edited by B. Asamoto (VCH, New York, 1991).
[2] L. K. Herold and R. T. Kouzes, Int. J. Mass Spectrom. Ion Processes **96**, 275 (1990).
[3] G. M. Alber, A.G. Marshall, N. C. Hill, L. Schweikhard, and T. L. Ricca, Rev. Sci. Instrum. **64**, 1845 (1993).
[4] P. A. Limbach, P. B. Grosshans, and A. G. Marshall, Anal. Chem. **65**, 135 (1993).
[5] C. D. Hanson, E. L. Kerley, M. E. Castro, and D. H. Russell, Anal. Chem. **61**, 2040 (1989).
[6] C. D. Hanson, M. E. Castro, and D. H. Russell, Anal. Chem. **61**, 2130 (1989).
[7] G. T. Uechi and R. C. Dunbar, J. Am. Soc. Mass Spectrom. **3**, 734 (1992).
[8] M. V. Gorshkov and E. N. Nikolaev, Int. J. Mass Spectrom. Ion Processes **125**, 1 (1993).
[9] T. M. O'Neil, Phys. Fluids **23**, 2216 (1980).
[10] T. M. O'Neil and R. A. Smith, Phys. Fluids B **4**, 2720 (1992).
[11] J. Notte, A. J. Peurrung, J. Fajans, R. Chu, and J. Wurtele, Phys. Rev. Lett. **69**, 3056 (1992).
[12] A. J. Peurrung and J. Fajans, Phys. Fluids B **5**, 4295 (1993).
[13] S. Guan, X. Xiang, and A. G. Marshall, Int. J. Mass Spectrom. Ion Processes **124**, 53 (1993).
[14] J. E. Bruce, G. A. Anderson, S. A. Hofstadler, B. E. Winger, and R. D. Smith, Rapid Commun. Mass Spectrom. **7**, 700 (1993).
[15] B. E. Winger, S. A. Hofstadler, J. E. Bruce, H. R. Udseth, and R. D. Smith, J. Am. Soc. Mass Spectrom. **4**, 566 (1993).
[16] J. H. Malmberg and J. S. deGrassie, Phys. Rev. Lett. **35**, 577 (1975).
[17] J. J. Bollinger, D. J. Heinzen, F. L. Moore, W. M. Itano, D. J. Wineland, and D. H. E. Dubin, Phys. Rev. A **48**, 525 (1993).
[18] J. B. Jeffries, S. E. Barlow, and G. H. Dunn, Int. J. Mass Spectrom. Ion Processes **54**, 169 (1983).
[19] R. W. Gould and M. A. LaPointe, Phys. Rev. Lett. **67**, 3685 (1991).
[20] R. W. Gould and M. A. LaPointe, Phys. Fluids B **4**, 2038 (1992).
[21] K. S. Fine, C. F. Driscoll, and J. H. Malmberg, Phys. Rev. Lett. **63**, 2232 (1989).
[22] R. S. VanDyck, R. L. Moore, D. L. Farnham, and P. B. Schwinberg, Phys. Rev. A **40**, 6308 (1989).
[23] R. C. Davidson, *Physics of Nonneutral Plasmas* (Addison-Wesley, Redwood City, CA, 1990), pp. 39–52.
[24] R. H. Levy, Phys. Fluids **8**, 1288 (1965).
[25] R. J. Briggs, J. D. Daugherty, and R. H. Levy, Phys. Fluids **13**, 421 (1970).
[26] A. J. Peurrung, J. Notte, and J. Fajans, J. Fluid Mech. **252**, 713 (1993).
[27] F. H. Laukien, Int. J. Mass Spectrom. Ion Processes **73**, 81 (1986).
[28] X. Xiang, P. B. Grosshans, and A. G. Marshall, Int. J. Mass Spectrom. Ion Processes **125**, 33 (1993).
[29] G. Gabrielse, L. Haarsma, and S. L. Rolston, Int. J. Mass Spectrom. Ion Processes **88**, 319 (1989).
[30] W. W. Yin, M. Wang, A. G. Marshall, and E. B. Ledford, J. Am. Soc. Mass Spectrom. **3**, 188 (1992).
[31] S. Kida, J. Phys. Soc. Jpn. **50**, 3517 (1981).
[32] D. J. Heinzen, J. J. Bollinger, F. L. Moore, W. M. Itano, and D. J. Wineland, Phys. Rev. Lett. **66**, 2080 (1991).
[33] A. J. Theiss, R. A. Mahaffey, and A. W. Trivelpiece, Phys. Rev. Lett. **35**, 1436 (1975).